SLAC-PUB-11985
July 2006

Interplay of the Chirps and Chirped Pulse Compression in a High-gain Seeded Free-electron Laser*

Juhao Wu,[1,†] J.B. Murphy,[2] P.J. Emma,[1] X.J. Wang,[2] T. Watanabe,[2] and Xinming Zhong[3]

[1] *Stanford Linear Accelerator Center, Stanford University, Stanford, CA 94309*
[2] *National Synchrotron Light Source, Brookhaven National Laboratory, Upton, NY 11973-5000*
[3] *Institute of Low Energy Nuclear Physics, Beijing Normal University, Beijing 100875, P. R. China*

(Dated: July 25, 2006)

In a seeded high-gain Free-electron Laser (FEL), where a coherent laser pulse interacts with an ultra-relativistic electron beam, the seed laser pulse can be frequency chirped, and the electron beam can be energy chirped. Besides these two chirps, the FEL interaction introduces an intrinsic frequency chirp in the FEL even if the above mentioned two chirps are absent. In this paper we examine the interplay of these three chirps. The problem is formulated as an initial value problem, and solved via a Green function approach. Besides the chirp evolution, we also give analytical expressions for the pulse duration and bandwidth of the FEL, which remains fully longitudinally coherent in the high gain exponential growth regime. Because the chirps are normally introduced for a final compression of the FEL pulse, some conceptual issues are discussed. We show that in order to get a short pulse duration, an energy chirp in the electron beam is necessary.

Submitted to Journal of the Optical Society of America B: Optical Physics

I. INTRODUCTION

In a seeded Free-electron Laser (FEL), a coherent laser interacts with an ultra-relativistic electron beam in an undulator. The FEL interaction induces an intrinsic frequency chirp in the FEL light. Besides this intrinsic frequency chirp, the seed itself can be frequency chirped, and the electron beam can be energy chirped. These three chirps compete with each other, and the interplay of these three chirps is studied in this paper. The problem is formulated as an initial value problem, and solved via a Green function approach. Such an approach [1, 2, 3, 4, 5, 6], has been used to study the so-called Self Amplified Spontaneous Emission (SASE) FEL [7]. Besides the chirp evolution, the pulse duration and bandwidth are also characterized. Indeed, the evolution of the pulse duration, the bandwidth, and the chirp develops in a fashion that the longitudinal emittance is preserved [8]. Beyond this direct application to the seeded high-gain FEL, the study in this paper falls into the more general interests of studying the charged particle interacting with a chirped electromagnetic wave [9].

The paper is organized as the follows. In Sec. II, we introduce the coupled Vlasov-Maxwell equations to describe the FEL interaction. We formulate the problem as an initial value problem and solve via a Green function approach. We then introduce the notation to describe a chirped seed laser pulse. These notations are later used for the FEL. With the solution of the FEL electric field, we compute the evolution of the pulse duration, the bandwidth, and the chirp of the FEL in Sec. III. Interesting physics about the interplay of the seed frequency chirp, the electron beam energy chirp, and the intrinsic FEL interaction induced frequency chirp is discussed in Sec. IV. The very purpose of the frequency chirped FEL is for a possible compression after the FEL light leaves the undulator, some conceptual issues regarding chirped pulse compression are explored in Sec. V. We show that in order to get FEL pulse duration shorter than the initial seed laser pulse duration, an energy chirp in the electron beam is necessary. We then give discussions and conclusion in Sec. VI.

II. VLASOV-MAXWELL ANALYSIS FOR AN INITIAL VALUE PROBLEM

To analyze the start-up of a seeded FEL amplifier we use the coupled set of Vlasov and Maxwell equations which describe the evolution of the electrons and the radiation fields. We follow the analysis and notation of Ref. [5]. Although we study a seeded FEL in this paper, part of the derivation is the same as for the SASE case [5]. We start from the point where the derivation for the seeded FEL is different from those for the SASE FEL.

For the seeded FEL, we start with Eq. (A9) of Ref. [5] and keep only the $A(\theta', 0)$, the initial field envelope term, to get,

$$f(\theta, s) = \int_{-\infty}^{\theta} d\theta' e^{-s(\theta-\theta')+\frac{i(2\rho)^3(\theta-\theta')}{(s-i\mu\theta)(s-i\mu\theta')}} A(\theta', 0). \quad (1)$$

The Laplace transform gives us the FEL field envelope

*The work of JW and PJE was supported by the US Department of Energy under contract DE-AC02-76SF00515. The work of JBM, XJW, and TW was supported by the US Department of Energy under contract DE-AC02-98CH10886 and the Office of Naval Research.

†Electronic address: jhwu@SLAC.Stanford.EDU

as

$$\begin{aligned} A(\theta,Z) &= \int_c \frac{ds}{2\pi i} e^{sZ} \\ &\times \int_{-\infty}^{\theta} d\theta' e^{-s(\theta-\theta')+\frac{i(2\rho)^3(\theta-\theta')}{(s-i\mu\theta)(s-i\mu\theta')}} A(\theta',0) \\ &\cong e^{\rho(\sqrt{3}+i)Z} \int_0^{\infty} d\xi A(\theta-\xi,0) e^{i\mu\theta(Z-\xi)} \\ &\times e^{-\rho(\sqrt{3}+i)\left[9(\xi-Z/3)^2/(4Z)\right]} e^{-i(\mu/2)(Z-\xi)\xi}, \end{aligned} \quad (2)$$

where we approximate the integral via a saddle point approach as in Ref. [5]. Obviously, once we know the initial seed field envelope $A(\theta,0)$, we can obtain the seeded FEL field envelope $A(\theta,Z)$ along the undulator. In the above equations, ρ is the Pierce parameter [7], $Z=k_w z$, $\theta=(k_0+k_w)z-\omega_0 t$, where $k_0=2\pi/\lambda_0$, $\omega_0=k_0 c$, and $k_w=2\pi/\lambda_w$ with λ_0 being the radiation wavelength, λ_w being the undulator period, and c being the speed of light in vacuum. Notice that [5],

$$\mu \equiv \frac{2}{\gamma_0\omega_0}\frac{d\gamma}{dt}, \quad (3)$$

characterizes the energy chirp in the electron beam with γ_0 being the resonant energy.

A. Green Function Bandwidth

In getting Eq. (2), we adopted the Green function [5],

$$g(Z,\theta;\mu) \cong e^{\rho(\sqrt{3}+i)Z} e^{-\rho(\sqrt{3}+i)[9(\theta-Z/3)^2/4Z]} e^{(i\mu/2)(Z-\theta)\theta}, \quad (4)$$

which gives an rms duration and an rms bandwidth of

$$\begin{cases} \sigma_{t,\mathrm{GF}}(z) = \frac{1}{\sqrt{3}\sigma_{\omega,\mathrm{GF}}(z)} \\ \sigma_{\omega,\mu,\mathrm{GF}}(z) = \sigma_{\omega,\mathrm{GF}}(z)\sqrt{1+\eta/9+\eta^2/81} \end{cases}, \quad (5)$$

where

$$\eta \equiv \frac{\mu k_w z}{\rho} = \frac{3\sqrt{3}\mu\omega_0^2}{\sigma_{\omega,\mathrm{GF}}^2(z)}, \quad (6)$$

and,

$$\sigma_{\omega,\mathrm{GF}}(z) \equiv \sqrt{\frac{3\sqrt{3}\rho\omega_0^2}{k_w z}}, \quad (7)$$

is the rms bandwidth of the FEL Green function for a coasting electron beam [1, 2, 3]. Notice that initially (at $z=0$), the Green function bandwidth is infinite. Also notice that, the Green function yields a duration independent of the energy chirp μ. As shown in Eq. (5), for the Green function to have a larger bandwidth, one needs to introduce a positive energy chirp ($\mu>0$) in the electron beam.

The Green function in Eq. (4) yields a phase as

$$\begin{aligned} \phi(t,z) = i\Bigg[&\left(1-3\rho-\frac{9\rho k_0}{4k_w}\right)k_0 z - \frac{1}{2}(k_0+k_w)k_0\mu z^2 \\ &+\left(k_0+\frac{k_w}{2}\right)\mu\omega_0 tz \\ &-\left(1-3\rho-\frac{9\rho k_0}{2k_w}\right)\omega_0 t - \frac{1}{2}\left(\mu+\frac{9\rho}{2k_w z}\right)\omega_0^2 t^2\Bigg]. \end{aligned} \quad (8)$$

The phase in Eq. (8) tells us that there is an intrinsic frequency chirp, which exists even for the electron beam not being energy chirped ($\mu=0$). This chirp for $\mu=0$ case is positive. In order to increase this intrinsic frequency chirp, one can introduce a positive energy chirp ($\mu>0$) in the electron beam.

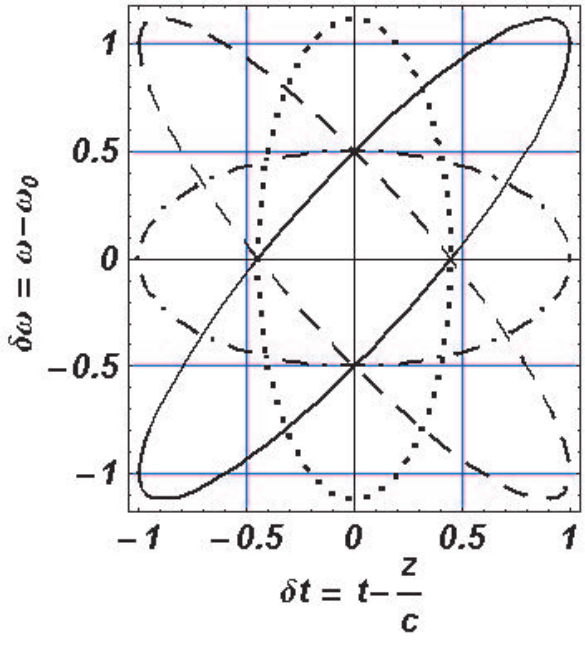

FIG. 1: Contour plot of the seed laser Wigner function $W_s(t-z/c,\omega-\omega_0)$. The solid ellipses is for $\alpha_0=1/4$ and $\beta_0=1/2$; the dashed ellipses for $\alpha_0=1/4$ and $\beta_0=-1/2$; dotted ellipse for $\alpha_0=5/4$ and $\beta_0=0$; and the dot-dashed ellipse for $\alpha_0=1/4$ and $\beta_0=0$.

The significance of the broadening of the Green function bandwidth and also the increasing of the intrinsic frequency chirp via a positive energy chirp in the electron beam ($\mu>0$ or $\eta>0$) as in Eqs. (5) and (8) is the following. As shown in Fig. 1, a light pulse is represented by an ellipse in the longitudinal phase space coordinates. If the light pulse is chirped, *i.e.*, the solid ellipse or the dashed ellipse, then the light pulse can be compressed to get a shorter pulse. Graphically, the pulse ellipse can be horizontally sheared to be compressed. To obtain a chirp in the seed laser, one can imagine shearing the ellipse vertically, or horizontally. A vertical shearing can be realized by a time lens [10, 11]. However, it is rather difficult to have a time lens in reality. In contrast to this

difficulty, a horizontal shearing can be realized by sending the laser pulse through a group velocity dispersive (GVD) medium. This horizontal shearing is relatively easy to do by a pair of gratings.

If the chirp is introduced by a horizontal shearing, *i.e.*, if the initial un-chirped pulse is the dotted ellipse, and the chirp is introduced by converting the dotted ellipse into the solid ellipse or the dashed ellipse; then the horizontal shearing to compress the pulse can at best recover the initial pulse duration, but never be able to get a shorter pulse than the initial un-chirped pulse (the dotted ellipse).

However, if the chirp is introduced by a vertical shearing, then the initial un-chirped pulse, *i.e.*, the dot-dashed ellipse, becomes the solid ellipse or the dashed ellipse. We can compress the chirped pulse by horizontal shearing, *i.e.*, the solid or the dashed ellipse becomes the dotted ellipse.

According to Eqs. (5) and (8), introducing a positive energy chirp in the electron beam ($\mu > 0$), the rms duration remains the same as that for $\mu = 0$. However, both the bandwidth and the chirp are increased. This is a vertical shearing, and is essential for chirped pulse compression. We will explore this in more details in Sec. V.

It is worth to point out that, in Ref. [6], the Green function was obtained in the regime

$$\frac{\mu k_w z}{\rho} \ll 1 \Longrightarrow \eta \ll 1. \tag{9}$$

B. Coherent Seed Laser Pulse

For a frequency chirped Gaussian seed laser pulse, the electric field of the seed laser is assumed to be,

$$E_s(t,z) = E_0 e^{i(k_0 z - \omega_0 t)} e^{-(\alpha_0 + i\beta_0)(t-z/c)^2}, \tag{10}$$

where E_0, k_0, ω_0, α_0 and β_0 characterize the peak field, the pulse wavenumber, frequency, duration, and chirp respectively. Notice that we introduce the chirp ($\beta_0 = d\omega/dt$) which is independent of the pulse duration [$\sigma_{t,\text{seed}} = 1/(2\sqrt{\alpha_0})$]. This is illustrated in Fig. 1. The un-chirped seed ($\beta_0 = 0$) is represented by the dot-dashed ellipse; and the chirped seed is either the solid ellipse or the dashed ellipse. The significance of this clarification will be detailed in Sec. V A.

To fully characterize the longitudinal properties of the seed pulse jointly in both the time and frequency domains, we introduce the Wigner distribution function [12, 13],

$$W(t,\omega,z) = \int E(t-\tau/2,z) E^*(t+\tau/2,z) e^{-i\omega\tau} d\tau. \tag{11}$$

With the Wigner function in Eq. (11), we can compute the expectation value and moments. As a matter of notation, in the following, any quantity $\langle \mathcal{F} \rangle$ means,

$$\langle \mathcal{F} \rangle \equiv \frac{\iint_{-\infty}^{\infty} dt d\omega W(t,\omega,z)\mathcal{F}}{\iint_{-\infty}^{\infty} dt d\omega W(t,\omega,z)}. \tag{12}$$

For the chirped Gaussian seed pulse of Eq. (10) the Wigner distribution function is given by,

$$W_s\left(t - \frac{z}{c}, \omega - \omega_0\right) = |E_0|^2 \sqrt{\frac{2\pi}{\alpha_0}} \times e^{-\frac{4\left(t-\frac{z}{c}\right)^2\left(\alpha_0^2+\beta_0^2\right) - 4\beta_0\left(t-\frac{z}{c}\right)(\omega-\omega_0)+(\omega-\omega_0)^2}{2\alpha_0}}. \tag{13}$$

Notice that the Wigner function is a function of $(t - z/c)$, a property of a travelling wave solution with constant velocity. The average values of t and ω of the seed laser are,

$$\begin{cases} \langle t \rangle \equiv \frac{z}{v_c} = \frac{z}{c} = \frac{z}{v_g} \\ \langle \omega \rangle = \omega_0 \end{cases}. \tag{14}$$

In this case, the centrovelocity v_c [14] is equal to the group velocity v_g of the pulse which in a vacuum is simply $v_c = v_g = c$. It will be seen in Sec. III B that the FEL interaction reduces the centrovelocity of the amplified seed laser pulse. The rms pulse duration and bandwidth of the seed laser are,

$$\begin{cases} \sigma_{t,\text{seed}} = \sqrt{\langle (t - \langle t \rangle)^2 \rangle} = \frac{1}{2\sqrt{\alpha_0}} \\ \sigma_{\omega,\text{seed}} = \sqrt{\langle (\omega - \langle \omega \rangle)^2 \rangle} = \sqrt{\frac{\alpha_0^2+\beta_0^2}{\alpha_0}} \end{cases}. \tag{15}$$

The cross moment $\langle (t - \langle t \rangle)(\omega - \langle \omega \rangle) \rangle$ can be determined from the Wigner function to be,

$$\langle (t - \langle t \rangle)(\omega - \langle \omega \rangle) \rangle = \frac{\beta_0}{2\alpha_0}. \tag{16}$$

The longitudinal emittance of a light beam is defined as,

$$\varepsilon_{\text{L}} \equiv \sqrt{\langle (t-\langle t \rangle)^2 \rangle \langle (\omega - \langle \omega \rangle)^2 \rangle - \langle (t - \langle t \rangle)(\omega - \langle \omega \rangle) \rangle^2}. \tag{17}$$

Substituting for the moments from the above equations it can be shown that $\varepsilon_{\text{L}} = 1/2$, the emittance of the seed light beam is equal to the minimum uncertainty value, *i.e.*, $\Delta t \Delta\omega \geq 1/2$, where the rms values are used for $\Delta t \equiv \sigma_t$ and $\Delta\omega \equiv \sigma_\omega$. This means that the light beam is fully longitudinally coherent, consisting of a single longitudinal mode, for all values of the chirp parameter. In Sec. III, we will show that when the seed laser is amplified in the FEL, it remains fully longitudinally coherent throughout the exponential gain regime.

In Fig. 1, we give four examples of a contour plot of the Wigner function ellipse for $W_s(t - z/c, \omega - \omega_0)$. The solid ellipse is for $\alpha_0 = 1/4$ and $\beta_0 = 1/2$; the dashed ellipse for $\alpha_0 = 1/4$ and $\beta_0 = -1/2$; the dotted ellipse for $\alpha_0 = 5/4$ and $\beta_0 = 0$; and the dot-dashed ellipse for $\alpha_0 = 1/4$ and $\beta_0 = 0$. The area of the ellipse (emittance) is the same in all cases. Notice that, the positively chirped case $\beta_0 > 0$, stands for the case where the tail ($\delta t > 0$) has higher frequency $\delta\omega > 0$.

C. FEL Field for a Gaussian Seed

For a Gaussian seed in Eq. (10), we write,

$$E(t,z=0)=E_0e^{-i\omega_0 t-(\alpha_0+i\beta_0)t^2}=E_0e^{i\theta-\frac{\theta^2}{\omega_0^2}(\alpha_0+i\beta_0)}. \tag{18}$$

Using notations in Ref. [5], *i.e.*, $E=Ae^{i(\theta-Z)}$, we have

$$A(\theta,0)=E_0e^{-\frac{\theta^2}{\omega_0^2}(\alpha_0+i\beta_0)}. \tag{19}$$

Therefore,

$$\begin{aligned}A(\theta,Z) &\cong E_0e^{\rho(\sqrt{3}+i)Z}\int_0^\infty d\xi e^{-\frac{(\theta-\xi)^2}{\omega_0^2}(\alpha_0+i\beta_0)}e^{i\mu\theta(Z-\xi)}\\ &\times e^{-\rho(\sqrt{3}+i)\left[9(\xi-Z/3)^2/(4Z)\right]}e^{-i(\mu/2)(Z-\xi)\xi}\\ &\cong E_{0,\mathrm{FEL}}e^{\frac{3}{4}\rho(\sqrt{3}+i)Z+i\mu\theta Z-\frac{\theta^2}{\omega_0^2}(\alpha_0+i\beta_0)}\\ &\times e^{-\frac{\left\{\frac{4i\theta}{\omega_0^2}(\alpha_0+i\beta_0)+\left[(Z+2\theta)\mu+3i\rho(\sqrt{3}+i)\right]\right\}^2}{\frac{16Z}{\omega_0^2}(\alpha_0+i\beta_0)+4\left[-2i\mu Z+9\rho(\sqrt{3}+i)\right]}Z},\end{aligned} \tag{20}$$

where we will not specify $E_{0,\mathrm{FEL}}$, since the normalization cancels out when computing the moments. Rewriting the electric field in the (t,z) coordinates gives,

$$\begin{aligned}E_{\mathrm{FEL}}(t,z) &= E_{0,\mathrm{FEL}}e^{\rho(\sqrt{3}+i)k_wz}\\ &\times e^{i(k_0z-\omega_0t)}e^{-[\alpha(z)+i\beta(z)](t-z/v_g)^2},\end{aligned} \tag{21}$$

with $\alpha(z)=1/[4\sigma_t(z)^2]$, $\beta(z)^2=\sigma_\omega(z)^2\alpha(z)-\alpha(z)^2$, and $\sigma_t(z)$ and $\sigma_\omega(z)$ are given in Eq. (23) in Sec. III B.

III. LIGHT EMITTANCE, LONGITUDINAL COHERENCE, AND PHASE SPACE

In order to compute moments of both time and frequency, we again introduce Wigner function for the FEL light as we did for the seed laser.

A. Wigner Distribution Function for FEL

The Wigner distribution function for the FEL electric field in Eq. (21) can be written as,

$$\begin{aligned}W(t,\omega,z)&\equiv\int_{-\infty}^{\infty}E_{\mathrm{FEL}}\Big(t-\frac{\tau}{2},z\Big)E^*_{\mathrm{FEL}}\Big(t+\frac{\tau}{2},z\Big)e^{-i\omega\tau}d\tau\\ &= E^2_{0,\mathrm{FEL}}e^{2\sqrt{3}\rho k_wz}\sqrt{\frac{2\pi}{\alpha(z)}}\\ &\times e^{-\frac{1}{2[1-r(z)^2]}\left\{\frac{\left[t-\frac{z}{v_c(z)}\right]^2}{\sigma_t^2(z)}-2r(z)\frac{\left[t-\frac{z}{v_c(z)}\right](\omega-\omega_s)}{\sigma_t(z)\sigma_\omega(z)}+\frac{(\omega-\omega_s)^2}{\sigma_\omega^2(z)}\right\}},\end{aligned} \tag{22}$$

where $r(z)$ is given in Eq. (25) in Sec. III B. Notice that the exponential growth of the radiation field can be suppressed in the Wigner function above in the analysis of the longitudinal phase space, since the moments are obtained by integration over t and ω, but not over z. Also notice that due to the energy chirp in the electron beam ($\mu\neq0$) even though we still have the combination of $t-z/v_c(z)$, $v_c(z)$ is now a function of z.

B. Pulse duration, bandwidth, and centrovelocity

Given the FEL electric field in Eq. (21), we can compute the FEL pulse duration and the bandwidth to be,

$$\begin{cases}\sigma_t(z) &= \Big(\Big[-4\beta_0\mu\omega_0^2+\mu^2\omega_0^4+3\sigma_{\omega,\mathrm{GF}}^4+4\alpha_0\sigma_{\omega,\mathrm{seed}}^2\\ &+ \left(6\alpha_0+2\sqrt{3}\beta_0-\sqrt{3}\mu\omega_0^2\right)\sigma_{\omega,\mathrm{GF}}^2\Big]\\ &/ \left\{3\sigma_{\omega,\mathrm{GF}}^2\left[-4\beta_0\mu\omega_0^2+\mu^2\omega_0^4\right.\right.\\ &+ \left.\left.4\alpha_0\left(\sigma_{\omega,\mathrm{GF}}^2+\sigma_{\omega,\mathrm{seed}}^2\right)\right]\right\}\Big)^{1/2}\\ \sigma_\omega(z) &= \frac{\sigma_{\omega,\mathrm{GF}}^3}{2\sqrt{3}}\Bigg[\Bigg(\frac{9\left[4\alpha_0\left(\sigma_{\omega,\mathrm{GF}}^2+\sigma_{\omega,\mathrm{seed}}^2\right)+\mu\omega_0^2\left(-4\beta_0+\mu\omega_0^2\right)\right]^2}{\sigma_{\omega,\mathrm{GF}}^4}\\ &+ \Bigg\{12\beta_0+\frac{2\mu\omega_0^2\left[4\alpha_0\sigma_{\omega,\mathrm{seed}}^2+\mu\omega_0^2\left(-4\beta_0+\mu\omega_0^2\right)\right]}{\sigma_{\omega,\mathrm{GF}}^4}\\ &+ \frac{\sqrt{3}\left[-\mu^2\omega_0^4+4\alpha_0\left(\sigma_{\omega,\mathrm{seed}}^2+\sqrt{3}\mu\omega_0^2\right)\right]}{\sigma_{\omega,\mathrm{GF}}^2}\Bigg\}^2\Bigg)\\ &/ \left(\left[4\alpha_0\left(\sigma_{\omega,\mathrm{GF}}^2+\sigma_{\omega,\mathrm{seed}}^2\right)+\mu\omega_0^2\left(-4\beta_0+\mu\omega_0^2\right)\right]\right.\\ &\times \Big[3\sigma_{\omega,\mathrm{GF}}^4+4\alpha_0\sigma_{\omega,\mathrm{seed}}^2-4\beta_0\mu\omega_0^2+\mu^2\omega_0^4\\ &+ \left.\sigma_{\omega,\mathrm{GF}}^2\left(6\alpha_0+2\sqrt{3}\beta_0-\sqrt{3}\mu\omega_0^2\right)\Big]\right)\Big]^{1/2}\end{cases}. \tag{23}$$

The cross moment can be determined from the Wigner function in Eq. (22) to be

$$\begin{aligned}&\langle(t-\langle t\rangle)(\omega-\langle\omega\rangle)\rangle\equiv\frac{\beta(z)}{2\alpha(z)} \qquad (24)\\ &= \frac{1}{6\sigma_{\omega,\mathrm{GF}}^2}\times\Big[4\sigma_{\omega,\mathrm{GF}}^2\left(3\beta_0\sigma_{\omega,\mathrm{GF}}^2+\sqrt{3}\alpha_0\sigma_{\omega,\mathrm{seed}}^2\right)\\ &+ 4\alpha_0\mu\left(3\sigma_{\omega,\mathrm{GF}}^2+2\sigma_{\omega,\mathrm{seed}}^2\right)\omega_0^2\\ &- \mu^2\left(8\beta_0+\sqrt{3}\sigma_{\omega,\mathrm{GF}}^2\right)\omega_0^4+2\mu^3\omega_0^6\Big]\\ &/ \left[4\alpha_0\left(\sigma_{\omega,\mathrm{GF}}^2+\sigma_{\omega,\mathrm{seed}}^2\right)+\mu\omega_0^2\left(-4\beta_0+\mu\omega_0^2\right)\right].\end{aligned}$$

The cross correlation coefficient, $r(z)$, is defined as,

$$r(z)\equiv\frac{\langle(t-\langle t\rangle)(\omega-\langle\omega\rangle)\rangle}{\sigma_t(z)\sigma_\omega(z)}. \tag{25}$$

Notice that even if $\beta_0=0$ and $\mu=0$, the cross coefficient, $r(z)$ in Eq. (25) is not equal to zero. This means that the FEL interaction introduces an intrinsic frequency chirp in the FEL. Notice that in the limit $z\to0$, the above expressions for the moments reduce to the expressions for the seed laser alone as given in Sec. II B.

Over the past 100 years a variety of definitions have been adopted to describe the velocity of an electromagnetic pulse traversing through a dispersive gain medium. Here, we use the centrovelocity [14], which is computed

to be

$$v_c^{-1}(z) \equiv \frac{\langle t\rangle}{z} = \left(k_0 + \frac{2}{3}k_w\right)/\omega_0 + \frac{\mu\omega_0 k_w\left(2\alpha_0 - 2\sqrt{3}\beta_0 + \sqrt{3}\mu\omega_0^2\right)}{2\sqrt{3}\left[4\alpha_0\left(\sigma_{\omega,\mathrm{GF}}^2+\sigma_{\omega,\mathrm{seed}}^2\right)-4\beta_0\mu\omega_0^2+\mu^2\omega_0^4\right]}. \quad (26)$$

The centrovelocity depends on z [15], because of the energy chirp in the electron beam ($\mu \neq 0$). For the un-chirped coasting beam case ($\mu = 0$), the second term in Eq. (26) is zero, and the FEL pulse has a constant centrovelocity, which is equal to the group velocity,

$$v_g \equiv \frac{\omega_0}{k_0 + \frac{2}{3}k_w}. \quad (27)$$

It is interesting to find that, even for $\mu \neq 0$, at $z = 0$, we have $v_c(z = 0) = v_g$, which is the group velocity for $\mu = 0$. The centrovelocity then deviates from the group velocity and evolves to its asymptote for $z \to \infty$. In this limit, $\sigma_{\omega,\mathrm{GF}}(z) \to 0$; and the centrovelocity defined in Eq. (26) becomes

$$v_c^{-1}(z\to\infty) \to v_g^{-1} + \frac{\mu\omega_0 k_w\left(2\alpha_0 - 2\sqrt{3}\beta_0 + \sqrt{3}\mu\omega_0^2\right)}{2\sqrt{3}\left[4\left(\alpha_0^2+\beta_0^2\right)-4\beta_0\mu\omega_0^2+\mu^2\omega_0^4\right]}. \quad (28)$$

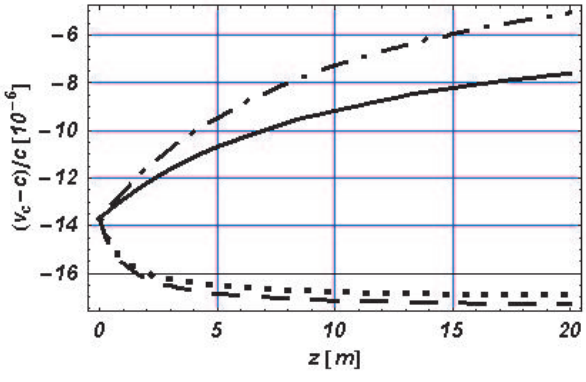

FIG. 2: Centrovelocity of the FEL with both an initial seed frequency chirp and an electron beam energy chirp for $z \in [0, 20]$ m and with $\rho = 10^{-3}$, $\lambda_0 = 0.8$ μm and $\lambda_w = 0.039$ m. The centrovelocity v_c is given in Eq. (26). The solid curve is for $\beta_0 > 0$ and $\mu > 0$; the dashed curve for $\beta_0 < 0$ and $\mu > 0$; the dotted curve for $\beta_0 > 0$ and $\mu < 0$; and the dot-dashed curve for $\beta_0 < 0$ and $\mu < 0$.

As an example, we take $\rho = 10^{-3}$, $\lambda_0 = 0.8$ μm and $\lambda_w = 0.039$ m, and set an initial frequency chirp in the seed laser to be $\beta_0 = \pm 1.0\times 10^{25}$; and also an energy chirp in the electron beam to be $\mu = \pm 2.0 \times 10^{-6}$. The results are shown in Fig. 2 for $z \in [0, 20]$ m. Interestingly, for our particular parameter set, the centrovelocity reaches its asymptote relatively sooner, if the two chirps have opposite sign. In Fig. 2, and all the other following plots, we take

$$\mu_{ap} \approx 2\rho/(\omega_0\sigma_t), \quad (29)$$

i.e., over σ_t, we introduce a relative energy chirp of ρ.

C. FEL Longitudinal Emittance and Longitudinal Coherence

The longitudinal emittance of the FEL light at any position, z, along the undulator is defined the same as in Eq. (17) but the $z-$dependent moments derived above must be used to obtain, $\varepsilon_{\mathrm{L}}(z) = 1/2$. The constancy of the emittance means that the amplified seed laser or FEL light remains fully longitudinally coherent throughout the exponential gain regime [8].

It can be seen from the formulae above, Eqs. (23) and (25), or Figs. 4 to 10, that the phase space begins with the characteristics of the seed laser and evolves as the FEL interaction modifies the pulse duration and the bandwidth; and imposes its own chirp on the FEL light. This evolution occurs in a fashion that preserves the area of the phase space ellipse and hence preserves the longitudinal coherence of the amplified seed light.

IV. INTERPLAY OF THE THREE CHIRPS

As we find above, the FEL interaction introduces an intrinsic frequency chirp on the FEL light; besides, the initial seed can have a frequency chirp, and the electron beam can have an energy chirp. Let us study the interplay of these three chirps. In the following Figs. 3 to 10, we choose a realistic FEL parameters set ($\rho = 10^{-3}$, $\lambda_0 = 0.8$ μm and $\lambda_w = 0.039$ m).

A. Intrinsic FEL chirp, *i.e.*, $\beta_0 = 0$ and $\mu = 0$

As the first example, we look at an un-chirped seed, *i.e.*, $\beta_0 = 0$, and the electron beam is also un-chirped, *i.e.*, $\mu = 0$. We find in Fig. 3 that, there is a small chirp developed in the FEL as shown in Eq. (25). According to our convention, the chirp is positive, *i.e.*, $\beta > 0$. So the tail ($\delta t > 0$) of the FEL has a higher frequency ($\delta\omega > 0$). This tells us that the electron beam together with the undulator is a GVD medium [8] with gain. In this particular example, we set $\alpha_0 = 1.4 \times 10^{24}$ s^{-2}. Notice that, it corresponds to the dot-dashed ellipse in Fig. 1. Therefore, in Figs. 3 to 9, we have the same α_0, *i.e.*, the same initial pulse duration.

B. Competition between the Seed Frequency Chirp and the FEL Intrinsic Chirp, *i.e.*, $\beta_0 \neq 0$ but $\mu = 0$

We introduce an initial frequency chirp ($\beta_0 = \pm 1.0 \times 10^{25}$ s^{-2}) in the seed laser, but the electron beam is

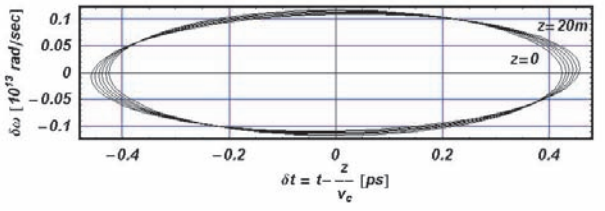

FIG. 3: Contour plot of the Wigner function $W(t-z/v_c, \omega-\omega_0)$ of the FEL light for $z \in [0, 20]$ m. The centrovelocity v_c is given in Eq. (26). The seed laser does not have a frequency chirp initially, nor does the electron beam have an energy chirp initially. In the plot, $\delta\omega = \omega - \omega_0$.

mono-energetic ($\mu = 0$). The ellipse evolution is displayed in Fig. 4 [1].

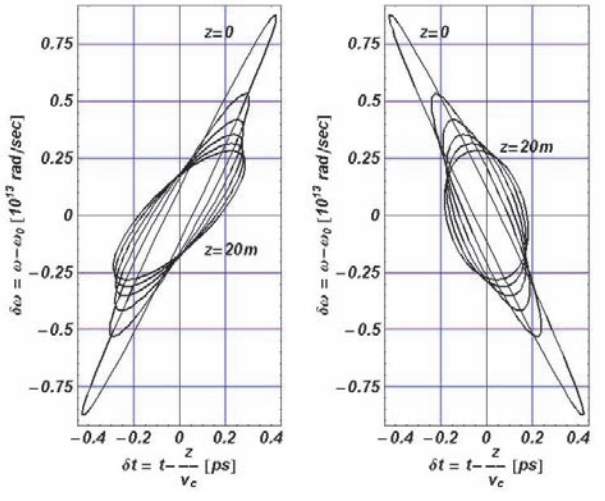

FIG. 4: Contour plot of the Wigner function $W(t-z/v_c, \omega-\omega_0)$ of the FEL light for $z \in [0, 20]$ m. The centrovelocity v_c is given in Eq. (26). The left/right plot is for an initial positive/negative seed laser frequency chirp of equal magnitude.

As we find out in Sec. IV A, the FEL interaction induced intrinsic frequency chirp is positive. Hence, we expect this intrinsic frequency chirp will compete with the initial negative chirp as shown in the right plot of Fig. 4. For the initially positively frequency chirped seed, the intrinsic frequency chirp will also shear the ellipse as shown in the left plot of Fig. 4. In Fig. 5, we display the pulse duration [σ_t], bandwidth [σ_ω], chirp [$\beta/(2\alpha)$], and longitudinal emittance [ε_L] versus the distance along the undulator. They are shown as the solid curves for $\beta_0 > 0$ and dashed curves for $\beta_0 < 0$.

As a comparison, there are also dotted curves, which stand for the evolution of the initially un-chirped seed, *i.e.*, the dotted ellipse in Fig. 1. We assume the frequency chirp in the seed is acquired by a horizontal shearing. As shown in the upper-left subplot of Fig. 5, even though the un-chirp seed has the shortest initial pulse duration, at about $z = 15$ m into the undulator, the initially negatively frequency chirped seed pulse becomes shorter than the initially un-chirped seed pulse, which is being stretched in the undulator. This is understandable, since the FEL intrinsic frequency chirp is positive, it cancels the initial negative frequency chirp, and makes the ellipse upright as shown in the right plot in Fig. 4.

[1] Notice that the same plots were shown as Fig. 1 in Ref. [8].

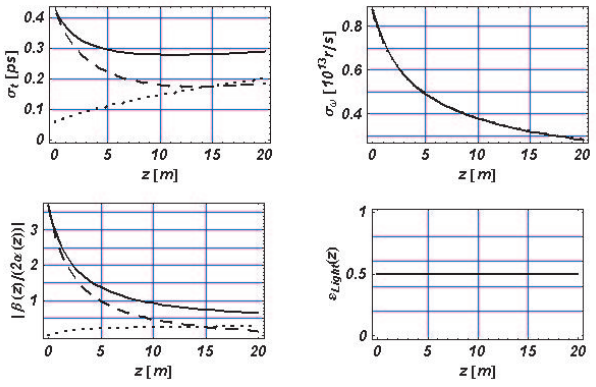

FIG. 5: Plot of the FEL pulse duration, bandwidth, chirp, and longitudinal emittance versus z for the same conditions as in Fig. 4. Notations are explained in the text.

It is worth to point out that for initial seed lasers having the same bandwidth, even though they can have different chirp, the evolution of the FEL bandwidth is the same as shown in the upper-right subplot of Fig. 5. Hence, in that subplot, the three curves lie on top of each other. Explicitly, the evolution of the FEL bandwidth is simplified from Eq. (23) to

$$\sigma_\omega(z)|_{\mu=0} = \frac{1}{\sqrt{\frac{1}{\sigma^2_{\omega,\text{seed}}} + \frac{1}{\sigma^2_{\omega,\text{GF}}(z)}}}. \tag{30}$$

This indicates that if we put aside the bandwidth reduction due to the FEL gain, the FEL process is a horizontal shearing like a GVD medium [8] if the electron beam is not energy chirped ($\mu = 0$).

C. Competition between the Energy Chirp and the FEL Intrinsic Frequency Chirp, *i.e.*, $\beta_0 = 0$ but $\mu \neq 0$

Having explored the case with a frequency chirped seed, we now look into the competition between the initial energy chirp in the electron beam and the intrinsic FEL frequency chirp.

In Fig. 3, we show the case where neither the electron beam is energy chirped, nor the seed laser is frequency chirped. We find that the FEL interaction developed a small positive frequency chirp. Let us introduce an energy chirp ($\mu = \pm 2.0 \times 10^{-6}$) in the electron beam, so that the Green function is changed. In Fig. 6, we show both the case of $\mu > 0$ and $\mu < 0$. The amount

of energy chirp we introduced is much larger than the intrinsic frequency chirp, hence the input energy chirp dominates.

The energy chirp is important, since it changes the Green function bandwidth and the intrinsic chirp as shown in Eqs. (5) and (8), while the initial seed frequency chirp does not change the Green function of the system.

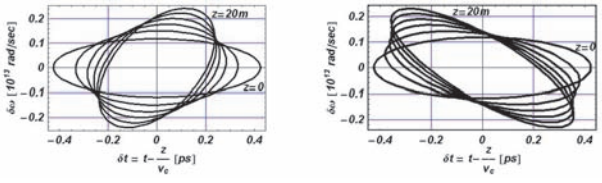

FIG. 6: Contour plot of the Wigner function $W(t-z/v_c, \omega-\omega_0)$ of the FEL light for $z \in [0, 20]$ m. The centrovelocity v_c is given in Eq. (26). The seed laser does not have a frequency chirp initially. The left/right plot is for an initial positive/negative electron beam energy chirp of equal magnitude. In the plot, $\delta\omega = \omega - \omega_0$.

D. Competition among the Seed Frequency Chirp, the Electron Beam Energy Chirp, and the FEL Intrinsic Frequency Chirp, *i.e.*, $\beta_0 \neq 0$ and $\mu \neq 0$

Let us look at the most complicated situation, *i.e.*, there is a frequency chirp ($\beta_0 = \pm 1.0 \times 10^{25}$ s^{-2}) in the seed laser, and also an energy chirp ($\mu = \pm 2.0 \times 10^{-6}$) in the electron beam. These two chirps together with the intrinsic FEL interaction induced frequency chirp will compete with each other.

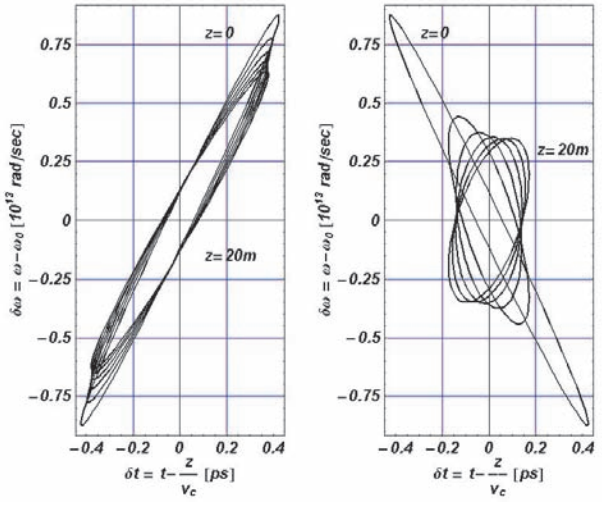

FIG. 7: Contour plot of the Wigner function $W(t-z/v_c, \omega-\omega_0)$ of the FEL light for $z \in [0, 20]$ m. The centrovelocity v_c is given in Eq. (26). The electron beam has a positive energy chirp. The left/right plot is for an initial positive/negative seed laser chirp of equal magnitude.

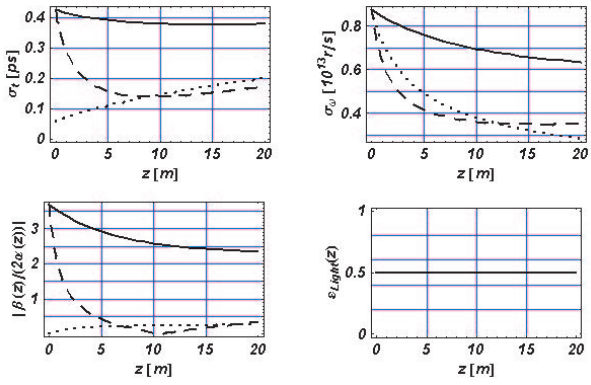

FIG. 8: Plot of the FEL pulse duration, bandwidth, chirp, and longitudinal emittance versus z for the same conditions as in Fig. 7. Notations are explained in the text.

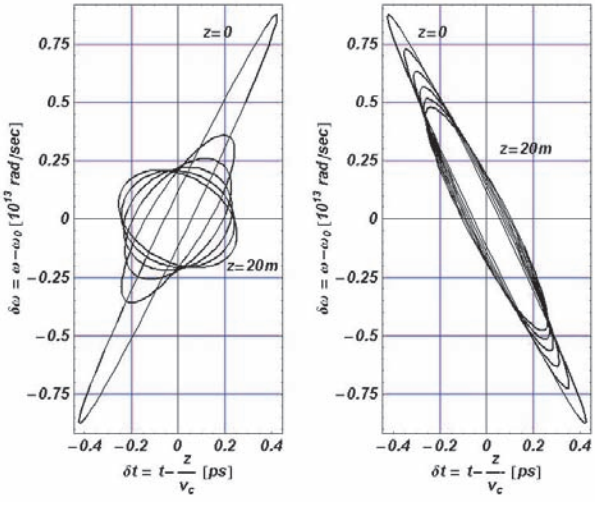

FIG. 9: Contour plot of the Wigner function $W(t-z/v_c, \omega-\omega_0)$ of the FEL light for $z \in [0, 20]$ m. The centrovelocity v_c is given in Eq. (26). The electron beam has a negative energy chirp. The left/right plot is for an initial positive/negative seed laser chirp of equal magnitude.

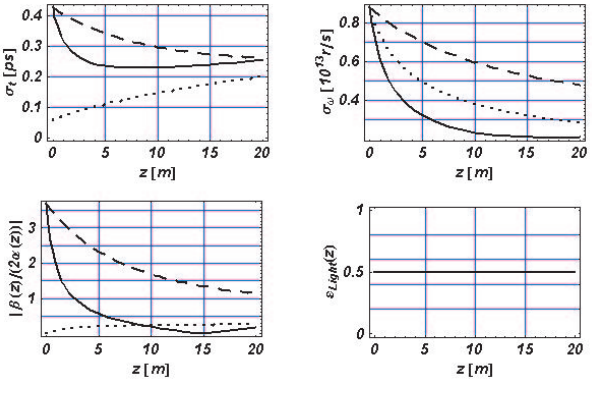

FIG. 10: Plot of the FEL pulse duration, bandwidth, chirp, and longitudinal emittance versus z for the same conditions as in Fig. 9. Notations are explained in the text.

It is interesting to observe the competition between the two input chirps, *i.e.*, the right plot of Fig. 7, and left plot of Fig. 9. In our particular examples, the energy chirp eventually wins over, since the final orientation of the ellipse approaches the electron beam energy chirp orientation ($\mu > 0$ for Fig. 7 and $\mu < 0$ for Fig. 9). Figures 7 and 9 should be compared with Fig. 4 to understand the role of the FEL interaction induced intrinsic frequency chirp. In our particular example, the effect from the intrinsic frequency chirp is less important. In Figs. 8 ($\mu > 0$) and 10 ($\mu < 0$), we display the pulse duration [σ_t], bandwidth [σ_ω], chirp [$\beta/(2\alpha)$], and longitudinal emittance [$\varepsilon_{\rm L}$] versus the distance along the undulator. The solid curves stand for $\beta_0 > 0$ and the dashed curves for $\beta_0 < 0$). For the parameter set which we choose here in this paper, due to the high-gain, the Green function property dominates over the initial seed condition. Again, as comparison, there are also dotted curves, which stand for the initially un-chirped seed, *i.e.*, the dotted ellipse in Fig. 1, evolves with an energy un-chirped electron beam. The dotted curves in Figs. 8 and 10 are the same as those in Fig. 5. One can find similar situation as for those in Fig. 5 except the different evolution of the bandwidth in the upper-right subplot of Figs. 8 and 10. One finds that the degeneracy is broken, and there is a possibility to get a larger bandwidth with an energy chirped electron beam.

V. CHIRPED PULSE COMPRESSION

Having explored the interplay of the three chirps, we now discuss some conceptual issues concerning chirped pulse compression.

A. Pre-undulator: the Initial Frequency Chirp in the Seed

In reality, the initial frequency chirp in the seed is introduced by passing the laser through a pair of dispersive gratings. Hence, when the frequency chirp is introduced, the pulse duration is also stretched. This is schematically shown in Fig. 1. The initially un-chirped seed is shown as the dotted ellipse, after traversing the gratings, a frequency chirp is introduced in the seed laser by stretching the pulse duration and this leads to the solid ellipse or the dashed ellipse depending on the chirp orientation.

When the seed laser traverses the pair of gratings to acquire a chirp, the rms spectral bandwidth $\sigma_{\omega,\rm seed}$ is kept the same. Hence, if the frequency chirped seed pulse is characterized by α_0, β_0, so that $\sigma_{\omega,\rm seed} = \sqrt{(\alpha_0^2+\beta_0^2)/\alpha_0}$ as shown in Eq. (15); then the initial seed before acquiring the chirp will have $\alpha_0 = \sigma^2_{\omega,\rm seed}$ and $\beta_0 = 0$. This is illustrated in Fig. 1. The dotted ellipse is the initial un-chirped seed ($\alpha_0 = 5/4$ and $\beta_0 = 0$). The chirp is acquired with $\sigma_{\omega,\rm seed}$ kept the same. The seed becomes the solid ellipse ($\alpha_0 = 1/4$ and $\beta_0 = 1/2$) or the dashed ellipse ($\alpha_0 = 1/4$ and $\beta_0 = -1/2$). We find that the chirp is introduced at the expense of stretching the seed pulse.

B. In the Undulator: Matching

The frequency chirped seed laser is then sent into the undulator to interact with an energy chirped electron beam. One should think of a "matched case", so that the final FEL will have the largest bandwidth. Therefore, the post-FEL grating pair can compress the FEL pulse mostly. As a first attempt, let us look at the resonance condition, so that initially the seed and the electron beam are matched, *i.e.*,

$$\frac{\gamma(t)^2}{\gamma_0^2} = \frac{\omega(t)}{\omega_0} \Longrightarrow \frac{d\gamma}{dt} \approx \frac{\gamma_0}{2\omega_0}\frac{d\omega}{dt} = \frac{\gamma_0\beta_0}{2\omega_0}. \tag{31}$$

According to Eq. (3), we then have

$$\mu_m \approx \frac{\beta_0}{\omega_0^2}. \tag{32}$$

Of course, the initial matching as expressed by Eq. (32) does not guarantee the final shortest pulse duration as we will discuss in detail in Sec. V D .

Let us recall the applicability of the theory in this paper. The Green function is obtained in the regime described by Eq. (9), which can be rewritten using Eq. (3) as

$$\frac{1}{\gamma_0}\frac{d\gamma}{dt}\frac{2\lambda_0\,(z/\lambda_w)}{c} \ll \rho. \tag{33}$$

Notice that the slippage time of the light pulse over the electron bunch after traversing a distance z in the undulator is $\tau_s \sim \lambda_0(z/\lambda_w)/c$. Hence, Eq. (33) tells us that the relative chirp over the slippage time $\tau_s(d\gamma/dt)/\gamma_0$ should be much smaller than ρ. Based on the same consideration, the applicability then requires

$$\beta_0 \ll \frac{\rho\omega_0^2}{k_w z}, \tag{34}$$

according to Eq. (9).

C. Post-undulator: Chirped Pulse Compression

After the FEL interaction in the undulator, the FEL light comes out with a frequency chirp, hence, we can send this chirped light through a pair of dispersive gratings to compressed the FEL pulse. This is done just in the opposite way (opposite sign GVD) as in the pre-undulator process. It is illustrated as the solid ellipse or the dashed ellipse evolves to the dotted ellipse in Fig. 1. Of course, the real ellipses are now the ellipses in Figs. 3 to 9.

D. Optimization

In order to optimize a possible experiment, let us summarize the results.

Assuming the initial unchirped seed laser to be Fourier-transform limited with a pulse duration of $\sigma_{t,i}$ resulting in a bandwidth of $\sigma_{\omega,\rm seed} = 1/(2\sigma_{t,i})$. Now assume the frequency chirp in the seed is $d\omega/dt = \beta_0$. The pulse is stretched to have an rms duration of $\sigma_{t,\rm seed} = 1/(2\sqrt{\alpha_0})$, with

$$\begin{aligned}\alpha_0 &= \frac{\sigma_{\omega,\rm seed}^2 + \sqrt{\sigma_{\omega,\rm seed}^4 - 4\beta_0^2}}{2} \\ &= \frac{1+\sqrt{1-64\beta_0^2\sigma_{t,i}^4}}{8\sigma_{t,i}^2},\end{aligned} \tag{35}$$

which is determined from Eq. (15). Notice that, in the limit of $\beta_0 \to 0$, we have $\alpha_0 \to 1/(4\sigma_{t,i}^2)$, so that $\sigma_{t,\rm seed} = \sigma_{t,i}$. Also notice that, $\beta_0 \le 1/(8\sigma_{t,i}^2)$. In the limit of $\beta_0 \to 1/(8\sigma_{t,i}^2)$, we have $\alpha_0 \to 1/(8\sigma_{t,i}^2)$, which leads to $\sigma_{t,\rm seed} = \sqrt{2}\sigma_{t,i}$. We are not so interested in the other solution

$$\alpha_0 = \frac{1-\sqrt{1-64\beta_0^2\sigma_{t,i}^4}}{8\sigma_{t,i}^2}. \tag{36}$$

This solution stands for the case in which the pulse has been stretched longer than the value determined by the largest $[\beta_0 \le 1/(8\sigma_{t,i}^2)]$, *i.e.*, $\sigma_{t,\rm seed} \ge \sqrt{2}\sigma_{t,i}$. The solution in Eq. (36), indicates the other limit of $\beta_0 \to 0$, *i.e.*, when $\beta_0 \to 0$, we have $\alpha_0 \to 0$, so that $\sigma_{t,\rm seed} \to \infty$.

Next, this frequency chirped seed laser (α_0 and β_0) interacts with the energy chirped electron beam (μ) in the undulator. The rms bandwidth $\sigma_\omega(z)$ along the undulator is given in Eq. (23). For the undulator length of z_w, the rms bandwidth for the FEL light is $\sigma_\omega(z_w)$ at the exit of the undulator.

Finally, this frequency chirped FEL light is compressed. Since it is fully longitudinally coherent, the final pulse duration is $\sigma_{t,f} = 1/[2\sigma_\omega(z_w)]$. This provides a direct relation between the final FEL pulse rms duration $\sigma_{t,f}$ and the initial seed laser pulse rms duration $\sigma_{t,i}$ via Eqs. (23) and (35).

According to Eqs. (9) and (34), we introduce

$$\epsilon \equiv \frac{3\sqrt{3}\beta_0}{\sigma_{\omega,\rm GF}^2} \qquad \text{and} \qquad \eta \equiv \frac{3\sqrt{3}\mu\omega_0^2}{\sigma_{\omega,\rm GF}^2}. \tag{37}$$

Notice that, η was introduced in Eq. (6). As we mentioned above, the final FEL pulse rms duration $\sigma_{t,f}$ and the initial seed laser pulse rms duration $\sigma_{t,i}$ directly relate as

$$\begin{aligned}\sigma_{t,f} &= \frac{1}{\sigma_{\omega,\rm GF}}\Big\{729\left[3\sqrt{3}\mathcal{B}\left(1+4\mathcal{C}^2\right)\right. \\ &+ \left. 8\mathcal{C}^4\eta(-4\epsilon+\eta)\right] \\ &\times \left\{\sqrt{3}\mathcal{B}\left(1+6\mathcal{C}^2\right) + \frac{8}{3}\mathcal{C}^4\left[81+\epsilon(18-4\eta)\right.\right. \\ &+ \left.\left.(\eta-9)\eta\right]\right\} \\ &/ \left(729\left[3\sqrt{3}\mathcal{B}\left(1+4\mathcal{C}^2\right)+8\mathcal{C}^4\eta(-4\epsilon+\eta)\right]^2\right. \\ &+ \left\{9\mathcal{B}\left[9+2\left(1+6\mathcal{C}^2\right)\eta\right]\right. \\ &+ \left.\left.\left. 8\sqrt{3}\mathcal{C}^4\left[324\epsilon-(9+8\epsilon)\eta^2+2\eta^3\right]\right\}^2\right)\Big\}^{1/2},\end{aligned} \tag{38}$$

where

$$\mathcal{B} = 3\sqrt{3} + \sqrt{27-64\epsilon^2\mathcal{C}^4} \quad \text{and} \quad \mathcal{C} = \sigma_{t,i}\sigma_{\omega,\rm GF}. \tag{39}$$

Let us first study the case of $\mu = 0$, *i.e.*, the electron beam is not energy chirped. In this case, we have

$$\sigma_{t,f}|_{\mu=0} = \frac{1}{2\sigma_\omega|_{\mu=0}} = \sigma_{t,i}\sqrt{1+\frac{1}{4\mathcal{C}^2}}, \tag{40}$$

where $\sigma_\omega|_{\mu=0}$ is given in Eq. (30). Equation (40) tells us that, without energy chirp in the electron beam ($\mu = 0$), the FEL process will unavoidably lengthen the pulse duration, even though the post-undulator pulse compression can partially cancel the pre-undulator pulse stretching. Notice that the result in Eq. (40) is rigorous.

According to Eqs. (9) and (34), we know $\epsilon \ll 1$ and $\eta \ll 1$. Hence, to obtain some insight to the case with an energy chirp ($\mu \neq 0$) in the electron beam, we expand Eq. (38) to the second-order in ϵ and η to get

$$\begin{aligned}\sigma_{t,f} &\approx \sigma_{t,i}\left[1+\frac{1}{4\mathcal{C}^2} - \frac{1+4\mathcal{C}^2}{36\mathcal{C}^2}\eta - \frac{4}{27}\mathcal{C}^2\epsilon\eta\right. \\ &- \left.\frac{1+2\mathcal{C}^2}{54}\eta^2 + \frac{2(3+4\mathcal{C}^2)}{243}\mathcal{C}^2\epsilon\eta^2 + \frac{16}{729}\mathcal{C}^6\epsilon^2\eta^2\right]^{1/2}.\end{aligned} \tag{41}$$

With the energy chirp ($\mu \neq 0$) in the electron beam, we find that the final pulse duration can be compressed more than the case of $\mu = 0$. This can be seen from the third and the fifth term in Eq. (41). A positive energy chirp ($\mu > 0$) will help more in compressing the pulse. Notice that, the first two terms in Eq. (41) are just those of Eq. (40).

We can introduce a frequency chirp ($\beta_0 \neq 0$) in the seed laser. The fourth term in Eq. (38) indicates that if the frequency chirp has the same sign as the energy chirp, the final pulse duration can be shorter. The sixth term tells us that a negative frequency chirp ($\beta_0 < 0$) helps to produce shorter pulse. This is due to the fact that the FEL intrinsic frequency chirp is positive. The seventh term indicates that introducing chirps will lengthen the pulse duration.

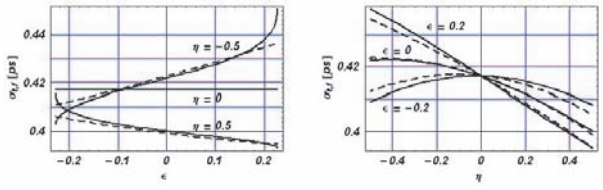

FIG. 11: Plot of the FEL pulse duration $\sigma_{t,f}$ after post-undulator pulse compression versus the dimensionless frequency chirp ϵ in the seed laser (left plot) and the dimensionless energy chirp η (right plot) in the electron beam introduced in Eq. (37).

To illustrate the situation discussed above, in Fig. 11. We take the realistic parameter set ($\rho = 10^{-3}$, $\lambda_0 = 0.8$ μm, $\lambda_w = 0.039$ m, and undulator length $z = 10$ m). The initial pulse duration is set to be $\sigma_{t,i} = 0.4$ ps. In the left plot, we show cases of electron beam with energy chirp ($\eta = \pm 0.5$) and without energy chirp ($\eta = 0$). For $\eta = \pm 0.5$, the solid curves are for the rigorous results given in Eq. (38), and the dashed curves are the approximated second-order results in Eq. (41). Indeed the second-order approximation is a reasonably good estimate. For $\eta = 0$, the final pulse duration is given in Eq. (40), *i.e.*, the FEL process lengthens the final pulse duration regardless of the frequency chirp (ϵ) in the seed laser. Figure 11 nicely illustrates the general features from Eq. (41), *e.g.*, to get shorter pulse, a positive energy chirp ($\eta > 0$) will help; the energy chirp and the frequency chirp having the same sign ($\epsilon\eta > 0$) helps. For a reasonably large positive energy chirp in the electron beam, and a positive frequency chirp in the seed laser, it is possible to get a shorter pulse duration than the initial seed pulse duration before pre-undulator process, *i.e.*, $\sigma_{t,f} < \sigma_{t,i}$. Recall that the initial pulse duration before pre-undulator process is $\sigma_{t,i} = 0.4$ ps. Similar information can be extracted from the right plot. When the seed laser is not frequency chirped ($\epsilon = 0$), a shorter pulse duration ($\sigma_{t,f}$) can be obtained by introducing a reasonably larger positive energy chirp ($\eta > 0$). The energy chirp and the frequency chirp having the same sign, *i.e.*, $\epsilon\eta > 0$, will help in producing a final short pulse duration. The solid curves are plotted using rigorous results in Eq. (38); and the dashed curves using the second-order approximation in Eq. (41).

According to Fig. 11, the matched condition introduced in Eq. (32) may not be the best solution after all, since Eq. (32) was based on only the initial condition. This is expected, due to the complicated interplay of the three chirps, and the fact that the FEL is a gain and dispersive medium.

VI. DISCUSSIONS AND CONCLUSIONS

The analysis in this manuscript is limited to the exponential gain regime before saturation. In general, for an FEL amplifier the output pulse duration, bandwidth and chirp will depend not only on the seed pulse duration, bandwidth and chirp but also on the seed amplitude as the amount of evolution of the phase space depends on how close to saturation the seed laser pulse is when it is injected into the FEL [8]. This will complicate more about the most appropriate energy chirp in the electron beam for a given set of FEL parameters, and the initial frequency chirp in the seed laser.

In summary, we have fully characterized the startup and evolution through the exponential gain regime of the field of an FEL amplifier in which a coherent frequency chirped seed pulse interacts with an energy chirped electron beam. We obtained explicit expressions for the pulse duration, bandwidth and chirp of the amplified light and we have shown that the light remains fully longitudinally coherent. We discuss in details about the interplay of the three chirps and further explore some conceptual issues about chirped pulse compression. We obtain a direct relation between the final FEL pulse duration $\sigma_{t,f}$ after post-undulator chirped pulse compression and the initial seed pulse duration $\sigma_{t,i}$ before acquiring frequency chirp. We find that an energy chirp in the electron beam is necessary, *i.e.*, we need $\mu \neq 0$, if we want $\sigma_{t,f} < \sigma_{t,i}$.

[1] J.-M. Wang and L.-H. Yu, "A transient analysis of a bunched beam free electron laser," Nuc. Instrum. and Methods in Physics Research A **250**, 484 (1986).

[2] K.J. Kim, "An analysis of self-amplified spontaneous emission," Nuc. Instrum. and Methods in Physics Research A **250**, 396 (1986).

[3] K.J. Kim, "Three-Dimensional Analysis of Coherent Amplification and Self-Amplified Spontaneous Emission in Free-Electron Lasers," Phys. Rev. Lett. **57**, 1871 (1986).

[4] K.J. Kim, "Temporal and transverse coherence of self-amplifed spontaneous emission," Lawrence Berkeley National Laboratory Report No. LBNL-40672 (1997).

[5] S. Krinsky and Z. Huang, "Frequency chirped self-amplified spontaneous-emission free-electron lasers," Phys. Rev. ST Accel. Beams **6**, 050702 (2003).

[6] E.L. Saldin, E.A. Schneidmiller, and M.V. Yurkov, "Self-amplified spontaneous emission FEL with energy-chirped electron beam and its application for generation of attosecond x-ray pulses," Phys. Rev. ST Accel. Beams **9**, 050702 (2006) .

[7] R. Bonifacio, C. Pellegrini, L.M. Narducci, "Collective instabilities and high-gain regime in a free-electron laser," Opt. Commun., **50**, 373 (1984).

[8] J.B. Murphy *et al.*, "Longitudinal-coherence preservation and chirp evolution in a high-gain laser-seeded free-electron-laser amplifier," Brookhaven National Laboratory Report No. BNL-75807-2006-JA, and Stanford Linear Acclerator Center Report No. SLAC-PUB-11852

(2006).
[9] A.G. Khachatryan, F.A. van Goor, and K.-J. Boller, "Interaction of free charged particles with a chirped electromagnetic pulse," Phys. Rev. E **70**, 067601 (2004).
[10] B.H. Kolner, "Space-time duality and the theory of temporal imaging," IEEE J. Quantum Electron. **30**, 1951 (1994).
[11] M. Nakazawa, H. Kubota, A. Sahara, and K. Tamura, "Time-domain ABCD matrix formalism for laser mode-locking and optical pulse transmission," IEEE J. Quantum Electron. **34**, 1075 (1998).
[12] E. Wigner, "On the quantum correction for thermodynamic equilibrium," Phys. Rev. **40**, 749 (1932).
[13] M.J. Bastiaans, "Propagation laws for the 2nd-order moments of the Wigner distribution function in 1st-order optical-systems," Optik **82**, 173 (1989).
[14] R.L. Smith, "Velocities of light," Am. J. Phys. **38**, 978 (1970).
[15] D. Anderson, J. Askne, and M. Lisak, "Wave packets in an absorptive and strongly dispersive medium," Phys. Rev. A **12**, 1546 (1975).